Available online at www.sciencedirect.com
SCIENCE DIRECT®
Biochemical and Biophysical Research Communications 309 (2003) 222–231
BBRC
www.elsevier.com/locate/ybbrc

Hypoxia induces apoptosis in SV40-immortalized rat proximal tubular cells through the mitochondrial pathways, devoid of HIF1-mediated upregulation of Bax

Tetsuhiro Tanaka,[a] Norio Hanafusa,[a] Julie R. Ingelfinger,[b] Takamoto Ohse,[a] Toshiro Fujita,[a] and Masaomi Nangaku[a,*]

[a] *Division of Nephrology and Endocrinology, University of Tokyo School of Medicine, 7-3-1, Hongo, Bunkyo-ku, Tokyo, Japan*
[b] *Division of Pediatric Nephrology, Massachusetts General Hospital, Boston, MA 02114, USA*

Received 28 July 2003

Abstract

Chronic hypoxia is a major contributor to tubulointerstitial injury in various renal diseases and apoptosis is apparently involved. Although many studies report hypoxia-induced apoptosis in cultured tubular cells, information has been limited in proximal tubular cells, those from the most susceptible portion of renal tubules against hypoxia. This study was to confirm a role for apoptosis in hypoxic proximal tubular cells and to investigate its association with HIF-1. Temperature-sensitive SV40-immortalized rat proximal tubular cells (IRPTCs) showed apoptosis in $21.9 \pm 2.9\%$ by hypoxia (0.2% O_2, 48 h), with alterations in mitochondrial signaling such as Bcl2 and caspase-9. Bax mRNA was unaffected during the process. However, treating IRPTCs at the nonpermissive temperature showed an upregulation of Bax by hypoxia, which was abrogated by overexpressing dominant-negative HIF-1α. These findings extend previous reports on hypoxia-mediated tubular cell apoptosis and demonstrate the possible involvement of HIF-1 as an upstream molecule of Bax.

Keywords: IRPTC; Bcl2; Caspase-9; p53

Tubulointerstitial injury is widely recognized as a hallmark of progressive renal disease, regardless of the etiology [1,2]. Chronic hypoxia, along with proteinuria, contributes greatly. Compromise of tubulointerstitial blood flow, directly or through endothelial injury and microvascular insufficiency, leads to chronic hypoxia in the tubulointerstitium, which ultimately results in tubular atrophy, leukocyte infiltration, deposition of extracellular matrix, and interstitial fibrosis [3]. Apoptosis in this context is a likely major candidate contributor to hypocellular tubulointerstitial fibrosis [4]. Currently, there are some reports documenting apoptotic tubular cell death following renal ischemic injury in vivo [5,6] and in vitro [7–9]. However, it also holds true that the behavior and susceptibility of cultured renal tubular cells in a hypoxic milieu differ to a significant degree according to which tubular segment they originate from [10]. Because of the limited availability of cultured renal proximal tubular cell lines, the assumed role for hypoxia during the execution of apoptosis has been still a matter of debate.

Apoptosis has two currently recognized distinct pathways of signal transduction, the mitochondrial pathways and the death receptor (Fas–FasL) pathways. Bcl2 is a major anti-apoptotic protein residing in the mitochondrial outer membrane [11]. It has been well characterized that Bcl2 protects cells against various types of apoptotic stimuli. Bax, on the other hand, is a pro-apoptotic member which exerts its function by homodimerizing with each other and accumulating in the mitochondrial membrane [12,13]. Presently, more than 30 proteins have been found to possess similar structures to Bcl2, thus forming the Bcl2 family [14–16]. Bcl2 family proteins mainly regulate mitochondrial membrane stability and cytochrome *c* release, and modulate

* Corresponding author. Fax: +81-3-5800-8806.
E-mail address: mnangaku-tky@umin.ac.jp (M. Nangaku).

0006-291X/$ - see front matter © 2003 Elsevier Inc. All rights reserved.
doi:10.1016/S0006-291X(03)01557-2

pro- and anti-apoptotic signals. Once the membrane stability is disrupted, cytochrome *c* released into the cytosol, in concert with ATP and Apaf1, activates caspase-9 and transduces its apoptotic signal.

Furthermore, as an upstream signaling of Bax, it is generally assumed that hypoxia stabilizes p53 [17] and leads cells to apoptosis through the enhanced expression of Bax [18–20] or other mechanisms [21], and hypoxia-inducible factor (HIF)-1 is most likely a candidate stabilizer of p53. However, the above process seems to depend on the cell types [22] or experimental conditions [23,24].

In this study, we took advantage of the employment of a temperature-sensitive SV40-immortalized rat proximal tubular cell line (IRPTC) and showed that hypoxia induces apoptosis in IRPTC through the mitochondrial pathways. Furthermore, we demonstrated that the execution is independent of the HIF-1- and p53-mediated elevation of Bax expression.

Materials and methods

Cell culture and induction of hypoxic environment. IRPTC is a cultured cell line derived from proximal tubular cells of male Wistar rats, immortalized by infection with the temperature-sensitive (ts) SV40 mutant viruses [25]. General characteristics of ts SV40 immortalized cell lines have been described elsewhere [26,27].

Cells were cultured in Dulbecco's modified Eagle's medium (Nissui Seiyaku, Tokyo, Japan) buffered with 25 mM Hepes (Sigma, St. Louis, MO) at pH 7.4 supplemented with 5% fetal bovine serum (JRH Biosciences, Lenexa, KS), 100 U/ml penicillin, 100 μg/ml streptomycin, and 0.01 mM nonessential amino acid, at 37 °C under a humidified atmosphere of 5%CO_2/95% air. In some specific experiments, cells were cultured at 40 °C to revert them to the untransformed phenotype.

Mild to moderate hypoxia (1% O_2) was provided by exposure to 1%O_2/5% CO_2 with the balance as nitrogen in a multi-gas incubator, APM-30D (ASTEC, Fukuoka, Japan). Severely hypoxic conditions were induced using anaerocult A mini (Merck, Darmstadt, Germany), which reduces the oxygen content to 0.2% within 1 h. Hypoxic stimulation was initiated at 70% confluence and IRPTCs were cultured in the culture medium containing 1% FBS during the treatment.

Detection of apoptosis. To detect and quantify apoptotic cells, we employed an annexin V binding assay [28]. Briefly, hypoxia-treated cells in 60-mm culture plates (Falcon, New Jersey, USA) were collected and double-stained with annexin V-FITC and propidium iodide (PI) utilizing annexin V-FITC Apoptosis Detection Kit (Medical and Biological Laboratories, Nagoya, Japan). Stained cells were processed by flow cytometry analysis (FACScan and LYSIS II software; both from Beckton–Dickinson, Franklin Lakes, NJ). The fraction of cells that was annexin V-positive and PI-negative was considered apoptotic.

In addition, we also quantified the number of apoptotic cells by terminal deoxynucleotidyl transferase (TdT)-mediated dUTP nick end labeling (TUNEL) method, as described elsewhere [29]. Cells were collected and fixed with 4% paraformaldehyde on ice for 10 min and reacted with TdT enzyme (Promega, Wisconsin, USA) at 37 °C for 1 h. Fluorescein-12-dUTP (Roche, Mannheim, Germany) was used as a substrate. After the reaction, cells were analyzed by flow cytometry. At least 10,000 cells per condition were analyzed on FACScan program.

To confirm the presence of apoptosis further, we checked the presence of DNA ladder formation. DNA samples were prepared according to the standard phenol/chloroform extraction and ethanol precipitation method. The chromosomal DNA was run on a 2% agarose gel, stained with ethidium bromide, and visualized under UV transillumination.

Quantification of Bcl2 and Bax mRNA by real-time PCR. The expression of Bcl2 and Bax mRNA was quantified by real-time PCR. Total RNA of IRPTC exposed to 0.2% O_2 for 0, 6, 12, 24, and 48 h, respectively, was extracted using ISOGEN (Nippon Gene, Tokyo, Japan). Aliquots of 1 μg RNA were reverse-transcribed at 42 °C for 1 h in a 20 μl reaction volume using ImProm-II Reverse Transcription System (Promega) and 1 μl of cDNA was used as a template for real-time PCR quantification. With the use of QuantiTest CYBR Green PCT Kit (Qiagen, California, USA), PCRs were performed on an iCycler (Bio-Rad, California, USA) under the following conditions; initial activation at 94 °C for 15 min, 40 cycles of amplification at 94 °C for 15 s, 55 °C for 30 s, and 72 °C for 30 s, followed by an additional data acquisition step provided by the supplier.

The standard curve method was employed to quantify the amount of each mRNA relative to the amount of β-actin in each reaction. The primers used here were as follows: Bcl2: forward 5′-CTGTGGATGA CTGAGTACCTGAAC-3′, reverse 5′-AGAGACAGCCAGGAGAA ATCAAAC-3′; Bax: forward 5′-TCATGAAGACAGGGGCCTTTT-3′, reverse 5′-CAATCATCCTCTGCAGCTCCA-3′; and β-actin: forward 5′-CTTTCTACAATGAGCTGCGTG-3′, reverse 5′-TCATGA GGTAGTCTGTCAGG-3′.

Measurement of mitochondrial membrane potentials and caspase-9 activity. To identify the involvement of changes in mitochondrial membrane potentials, membrane potentials were measured with flow cytometry. Hypoxia-treated cells were collected and incubated with 10 μM rhodamine-123 (Wako) for 15 min, which were subsequently double-stained with 10 μM PI.

Caspase-9 activity was measured using a Colorimetric Assay Kit (MBL). In brief, hypoxia-treated cells were collected and suspended in cell lysis buffer. Aliquots of 200 μg protein were incubated in reaction buffer containing 10 mM DTT at 37 °C for 1 h. Two hundred micromolar ρ-nitroaniline (ρ-NA)-conjugated LEHD (LEHD-ρ-NA) was used as a substrate. By measuring the optic absorbance at 405 nm with a microtiter plate reader, the relative caspase-9 activity was calculated.

Establishment of stable transfectants overexpressing Bcl2, HIF-1α, and dominant-negative HIF-1α. To clarify the cytoprotective effect of Bcl2 in the context of hypoxia-induced cell injury, we constructed stable transfectants overexpressing rat Bcl2.

An open reading frame coding for the rat Bcl2 was obtained by RT-PCR using total RNA of Lewis rat kidney as a template. Primers used were forward 5′-GCCACCATGGCGCAAGCCGGGAGAAC-3′ and reverse 5′-GCTCTAGATCACTTGTGGCCCAGGTATG-3′, respectively.

The PCR fragment of 725 nt was subcloned into pCR2.1 (Invitrogen, San Diego, CA) and was processed to dideoxy-DNA sequencing. The sequence-confirmed fragment was digested with *Eco*RI and again incorporated to the mammalian expression vector, pcDNA3.1(−) (Invitrogen). Then, the vector plasmid (pcDNA-Bcl2) was stably transfected to IRPTC using Lipofectamine reagent (Gibco Life Technologies) according to the manufacturer's protocol. Outgrowths of cells carrying pcDNA-Bcl2 were isolated using cloning cylinders and selected in the culture medium containing 600 μg/ml geneticin (Sigma) and maintained at 200 μg/ml.

Expression vectors coding for HIF-1α and dominant-negative (dn) HIF-1α were prepared as previously described [30] using the following primers; HIF-1α: forward 5′-GGAAGACAACGCGGGCAC-3′, reverse 5′-GGAGCTGTGAATGTGCTGTGATCTGGC-3′ and dnHIF-1α: forward 5′-CCGCTCGAGACCATGCGAAGCAAAGAGTCT G-3′, reverse 5′-GGGGTACCTCACTTATCAAAAAGGCAG CT-3′. An open reading frame coding for the dn HIF-1α is a 1.1 kb fragment whose product lacks both the DNA binding and transactivation domain. In both cases, RNA out of a C57BL/6J mouse kidney was used as a template.

Antisense treatment of Bax. To confirm the pro-apoptotic role for Bax, we inhibited its function by introducing antisense oligonucleotides (ODNs). Phosphorothioated antisense ODN (5′-TGCTCCC CGGACCCGTCCAT-3′) was designed as previously described [31]. In parallel, sense ODN (5′-ATGGACGGGTCCGGGGAGCA-3′) was used as a control. IRPTCs seeded in 96-well culture plates were transfected with these ODNs at 1 μM using cationic liposome. Forty-eight hours after transfection, cells were subjected to hypoxic treatment. The proportion of dead cells was measured by LDH-release assays.

Immunoblotting and immunocytochemistry. For the quantitative comparison of Bcl2, Bax, and p53, Western blotting was performed. Forty micrograms of whole cell lysate was separated by SDS–PAGE under reducing conditions. After the electrophoresis, samples were transferred to polyvinylidine difluoride (PVDF) membranes (Millipore, Japan) and developed with mouse monoclonal anti-Bcl2 antibody (Santa-Cruz biochemistry, California, USA) at 1:100, rabbit polyclonal anti-Bax antibody (Santa-Cruz biochemistry) at 1:200 or mouse monoclonal anti-p53 antibody (Calbiochem, California, USA) at 1:10, followed by incubation with alkaline phosphatase-conjugated anti-mouse/rabbit IgG (Promega) at 1/1000. BCIP/NBT tablets (Sigma) were used as a substrate. CBB staining of the membranes confirmed equal loading and transfer.

The localization and translocation of Bax was examined by double staining with Mitotracker (Molecular Probes, Oregon, USA). Cells on 4-well Lab-Tek chamber slides (Nalge Nunc International, Illinois, USA) were cultured under hypoxic conditions and labeled with MitoTracker for 30 min. Samples were fixed with ice-cold methanol/acetone and incubated with anti-Bax antibody at 1/100, biotinylated anti-mouse IgG (Vector) at 1/400, and Oregon Green 488 streptavidin (Molecular Probes) at 1/400. Slides were observed with a microscope equipped with fluorescein filters (Olympus, Tokyo, Japan). For negative controls, samples were processed without the incubation step with the primary antibody.

Transient transfection assay. The functional analysis of HIF-1 activity in control IRPTCs and stable clones with HIF-1α or dnHIF-1α was performed by dual-luciferase assays. Briefly, 1.0×10^5 of IRPTCs in 24-well culture dish was transfected with 500 ng of the luciferase reporter vector under the control of hypoxia-responsive elements (HREs) of the rat VEGF gene [32] and 25 ng of pRL-CMV (Promega) using cationic liposome. Twenty-four hours after transfection, cells were subjected to hypoxic stimulation of indicated oxygen content and duration. After treatment, cells were lysed with 100 μl of passive lysis buffer and assayed for firefly and renilla luciferase activity using the picagene dual-assay system (Toyo ink, Tokyo, Japan). A Lumat 9507 luminometer (EG and Berthold) was used for the measurement.

Statistical analysis. Stat View Version 5.0 (SAS Institute, Cary, NC) was used for statistical analysis. The data were compared using unpaired Student's t test with the correction by Bonferroni/Dunn's method and expressed as means ± SEM. p values of <0.05 were defined as statistically significant.

Results

Severe hypoxia induces apoptosis in IRPTC

First, we tested the hypothesis that the hypoxic ambience induces apoptosis in cultured renal proximal tubular cells. As seen in Fig. 1A, IRPTC exposed to hypoxia at two different levels of severity (0.2% and 1% O_2) showed a time-dependent increase in the number of apoptotic cells, according to the annexin V binding assay. When IRPTCs were cultured in 0.2% O_2 for 48 h, $21.9 \pm 1.9\%$ of cells was classified as apoptotic, as compared to $3.9 \pm 0.3\%$ under normoxic control conditions ($p < 0.0001$). In 1% O_2, on the other hand, the proportion of apoptotic cells showed a more gradual increase ($7.8 \pm 1.0\%$ at 48 h as compared to $3.9 \pm 0.3\%$ in controls, $p = 0.0013$).

The TUNEL assay revealed similar trends (Fig. 1B). The proportion of cells determined to be apoptotic was $12.3 \pm 0.8\%$ in 0.2% O_2 ($p = 0.0045$) and $6.3 \pm 2.5\%$ in 1% O_2 ($p = 0.1437$) at 48 h, respectively, as compared to $2.7 \pm 0.7\%$ in control. There was a good correlation in the detection of apoptosis between TUNEL (x) and annexin V (y) binding assays ($y = 1.53x - 0.29$, $r^2 = 0.9466$).

Furthermore, when we examined the cells for the presence of internucleosomal DNA fragmentation, a molecular characteristic appearing in the final stage of apoptotic cascade, a characteristic 180 bp DNA ladder pattern was detected in cells exposed to 0.2% O_2 for 48 h, but not in control cells (Fig. 1C).

In our experimental conditions, reoxygenation of 2–18 h following hypoxic stimulation did not alter the apoptosis profile (data not shown).

Cellular expression of Bcl2 and Bax, on exposure to severe hypoxia, and subsequent changes in mitochondrial membrane potentials

We next measured the cellular expression of Bcl2 and Bax, anti- and pro-apoptotic genes, respectively, after hypoxic stimulation. IRPTCs were cultured in 0.2% O_2 for up to 48 h. Our real-time PCR demonstrated that Bcl2 mRNA expression began to fall at 12 h, reaching 0.13 ± 0.01-fold at 48 h ($p = 0.0002$), while that of Bax remained at the same level throughout the hypoxic exposure (Figs. 2A and B). We calculated the Bax/Bcl2 ratio, an indicator of mitochondria-mediated apoptotic cell death. It began to rise at 12 h and reached 5.7-fold at 48 h compared to normoxic control (Fig. 2C).

During the process of apoptosis, the decrease in mitochondrial membrane potentials was observed by FACS analysis at 24 h and was more apparent with longer hypoxic stimulation (Fig. 3).

Overexpression of Bcl2 ameliorates hypoxia-induced apoptosis with reduction of caspase-9 activity

In order to elucidate the cytoprotective role that Bcl2 is expected to confer, we constructed stable transfectants overexpressing Bcl2. Western blotting analysis showed an increased expression of the Bcl2 protein in stable clones at any O_2 concentration tested (Fig. 4A). The Bcl2 bands in control IRPTCs showed an obvious decrease in its intensity as the ambient O_2 levels decreased, a consistent finding with the quantitative real-time PCR quantification of Bcl2 mRNA.

We then subjected IRPTCs overexpressing Bcl2 to hypoxic treatment. When cells were incubated in 0.2%

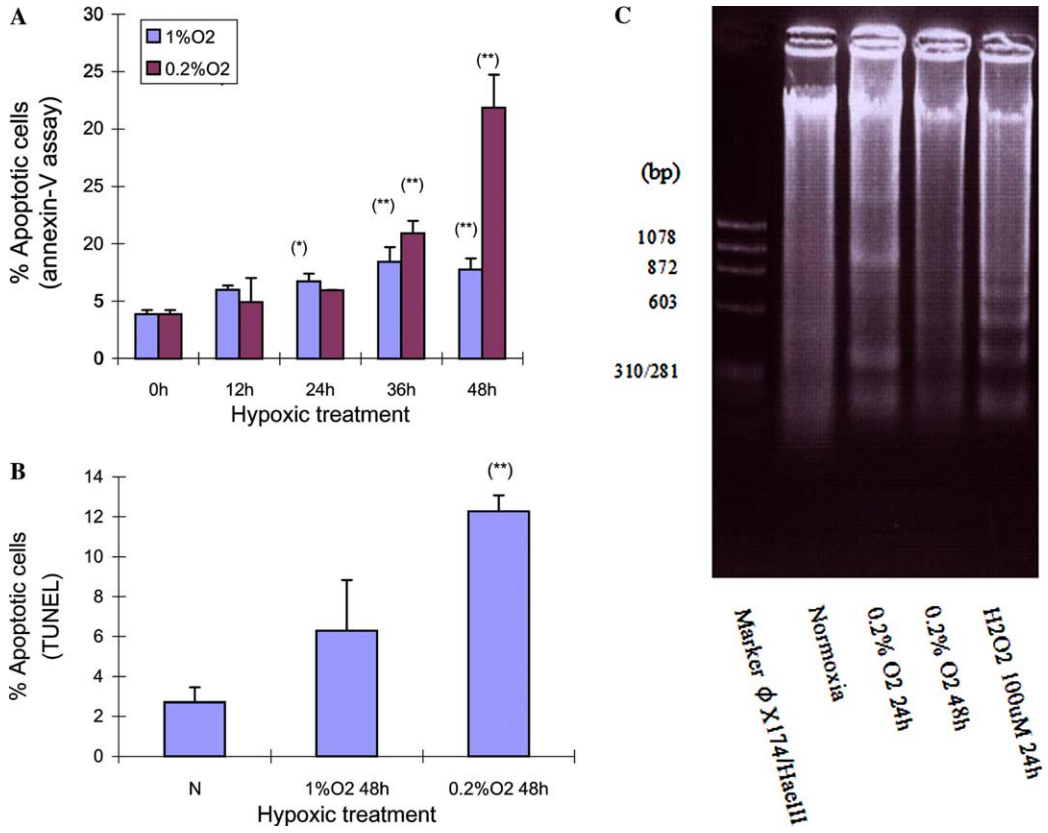

Fig. 1. Hypoxia induces apoptosis in IRPTC in a time-dependent manner. (A) IRPTCs exposed to two different severity of hypoxia (0.2% and 1% O_2) showed a time-dependent increase in the number of apoptotic cells (annexin V binding assay). When cultured in 0.2% O_2 for 48 h, $21.9 \pm 1.9\%$ of IRPTCs was classified as apoptotic, compared with $3.9 \pm 0.3\%$ in normoxic control. In mild to moderate hypoxia (1% O_2), the proportion of apoptotic cells showed a more gradual increase ($7.8 \pm 1.0\%$ at 48 h vs $3.9 \pm 0.3\%$ in control) ($n = 4$, $^{*}p < 0.05$, $^{**}p < 0.01$ vs normoxic control, respectively). (B) Percentage of apoptotic cells as measured by TUNEL assay. The proportion of cells determined to be apoptotic was $12.3 \pm 0.8\%$ in 0.2% O_2 and $6.3 \pm 2.5\%$ in 1% O_2 at 48 h, respectively, compared with $2.7 \pm 0.7\%$ in control ($n = 3$, $^{**}p < 0.01$ vs normoxic control). (C) Internucleosomal DNA fragmentation following hypoxic treatment. In samples undergoing hypoxia (0.2% O_2) for up to 48 h, a 180 bp DNA ladder pattern characteristic of apoptosis appeared, which was absent in normoxic controls. The rightmost lane represents the positive control by hydrogen peroxide (100 μM, 24 h).

O_2 for 48 h, $7.3 \pm 0.1\%$ of stable transfectants proceeded to apoptosis as compared to $21.9 \pm 2.9\%$ in control IRPTCs ($p < 0.0001$) (Fig. 4B), showing that overexpression of Bcl2 renders a consistent anti-apoptotic effect against hypoxia.

We further measured the activity of the signaling molecule located downstream of mitochondrial damage, caspase-9 (Fig. 4C). In control IRPTCs, the relative caspase-9 activity rose to $450 \pm 35\%$, as compared with $275 \pm 47\%$ in Bcl2-overexpressing clones ($p = 0.028$). This further supported the view that IRPTC apoptosis induced by hypoxia is mediated, at lease in part, through the mitochondrial signaling pathways and that Bcl2 plays a pivotal role upstream of caspase-9.

Antisense treatment of Bax reduces hypoxia-mediated IRPTC injury

The consistent anti-apoptotic effect conferred by Bcl2 stimulated us to determine the pro-apoptotic role for Bax by introducing antisense oligonucleotides (ODNs). After 48 h of antisense ODN delivery, the amount of Bax protein was reduced to a significant degree, whereas it was unaffected in sense ODN group (Fig. 5A).

Using these ODNs, we examined the possible cytoprotective effect by inhibiting Bax expression. As seen in Fig. 5B, results of LDH assays showed that treatment with antisense ODN resulted in a reduction in the number of dead cells ($65.0 \pm 1.0\%$), as compared to control ($76.1 \pm 3.2\%$, $p = 0.043$) and sense ODN ($79.3 \pm 2.6\%$, $p = 0.0005$) groups. Based on these observations, we concluded that Bax, along with Bcl2, plays a certain role in hypoxia-induced tubular cell apoptosis, although the amount of Bax mRNA was unaffected throughout the hypoxic treatment (Fig. 2B). In support of this conclusion, immunohistochemistry in Fig. 5C showed that Bax in the cytosol was translocated to mitochondria by hypoxic treatment.

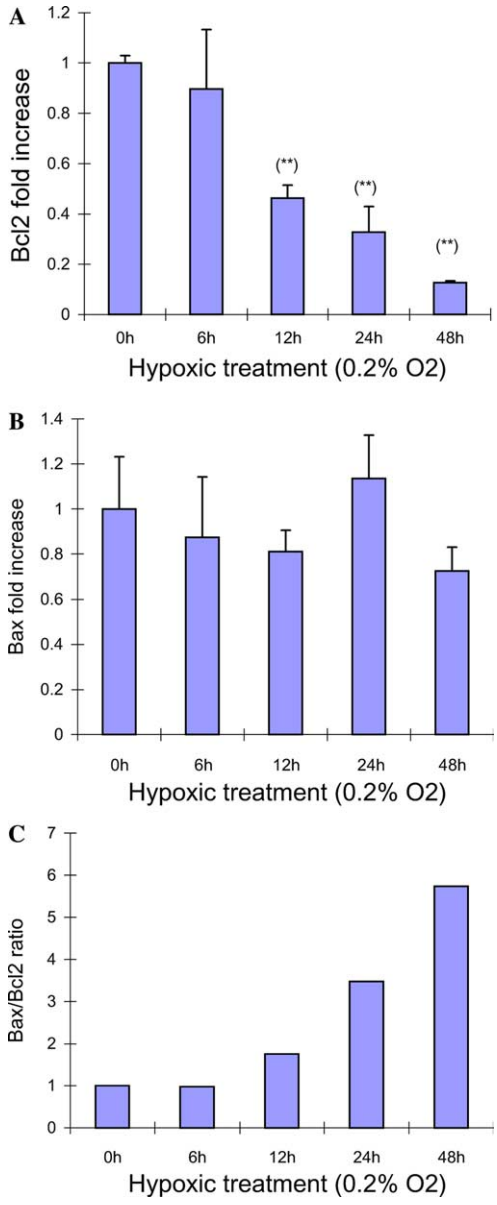

Fig. 2. Cellular expression of Bcl2 and Bax on exposure to hypoxia. (A) When IRPTCs were cultured in 0.2% O_2 for up to 48 h, the cellular mRNA expression of Bcl2 began to fall at 12 h, reaching below 1/10 of normoxic control (measured by real-time PCR). (B) While that of Bax remained at the same level throughout the hypoxic treatment. (C) The Bax/Bcl2 ratio, as an indicator of mitochondria-mediated apoptotic cell death, was calculated. It began to rise at 12 h of hypoxic treatment and reached 5.7-fold at 48 h compared to normoxic control ($n = 4$, $^{**}p < 0.01$ vs normoxic control).

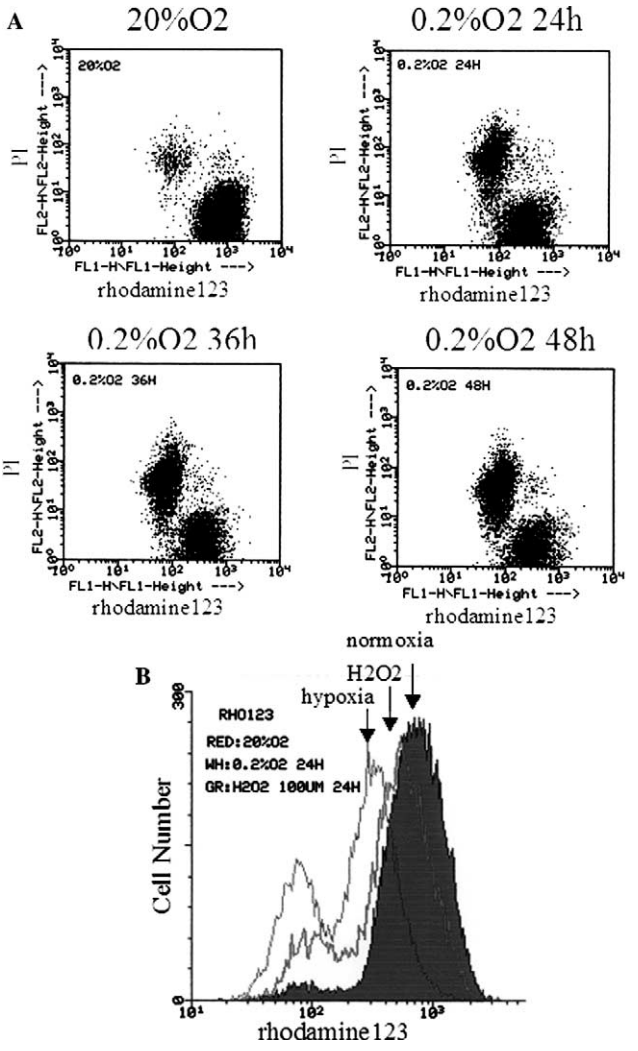

Fig. 3. Changes in mitochondrial membrane potentials. (A) Following hypoxic treatment, IRPTCs were double-stained with rhodamine-123 and PI as described. During hypoxic treatment, the decrease in mitochondrial membrane potentials was apparent through FACS analysis at 24 h and was more prominent with longer hypoxic incubation (parameters: FL1 for rhodamine-123, FL2 for PI). (B) A histogram of mitochondrial membrane potentials, as measured by rhodamine-123 uptake, is presented in a merged view. After 24 h of hypoxic treatment, the distribution of rhodamine-123 uptake is approximately the same as that of positive control. (representative of duplicate experiments performed independently).

HIF-1 is induced in IRPTC by hypoxia, but does not affect Bax mRNA expression and the resultant cell death

Furthermore, we wished to gain some insight into the upstream signaling of Bax. Currently, there is a widely recognized concept that HIF-1 stabilizes p53, which resultantly transactivates Bax transcription, although it seems to depend on the cell types or experimental conditions. In this regard, we tried to investigate the possible role of HIF-1 in hypoxia-induced IRPTC apoptosis.

First, we checked to see if IRPTC induces HIF-1α in severely hypoxic conditions we employed. Fig. 6A shows the relative luciferase activity in normoxic and hypoxic IRPTCs. An HRE-driven luciferase activity was increased by severe hypoxia (2.4 ± 0.1-fold) at 6 h, indicating that HIF-1 is activated in 0.2% O_2 in IRPTC. In parallel, we constructed stable clones carrying HIF-1α and dominant-negative (dn) HIF-1α to provide a more solid evidence on the role of HIF-1 in Bax transcription.

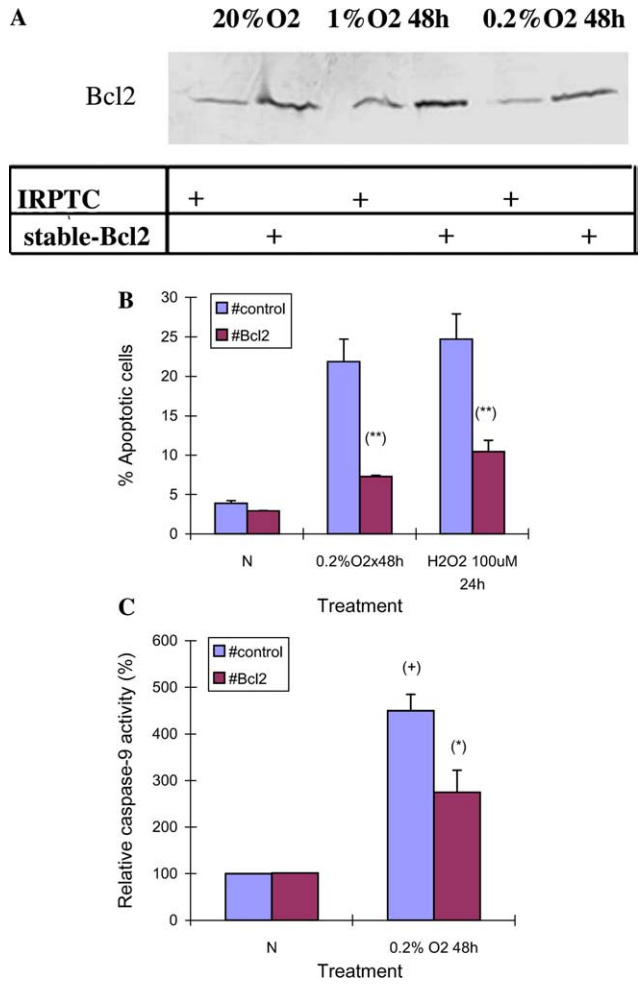

Fig. 4. Cytoprotective effect of Bcl2 on hypoxia-induced tubular cell injury. (A) Western blot analysis. The relative overexpression level of Bcl2 in Bcl2-overexpressing clones was confirmed by Western blotting. Stably transfected clones showed an apparently stronger band of Bcl2 than control IRPTCs at any O_2 concentration tested. Also of note is that the Bcl2 bands in control IRPTCs showed an obvious decrease in its intensity as the ambient O_2 levels decreased. (B) Anti-apoptotic effects of Bcl2 measured by annexin V binding assays. Stable transfectants incubated in 0.2% O_2 for 48 h showed $7.3 \pm 0.1\%$ of apoptotic cells as compared with $21.9 \pm 2.9\%$ in control IRPTCs (center, $n = 3$, $^{**}p < 0.01$ vs control IRPTCs). A similar anti-apoptotic effect was observed when we stimulated IRPTCs by hydrogen peroxide (left, 100 μM, 24 h). (C) Measurement of caspase-9 activity. The relative caspase-9 activity rose to $450 \pm 35\%$ in control IRPTCs, while that in stable transfectants was $275 \pm 47\%$ ($n = 4$, $^{+}p < 0.01$ vs unstimulated control, $^{*}p < 0.05$ vs control IRPTCs). These results imply that hypoxia induces apoptosis in IRPTC through the mitochondrial pathways and that Bcl2 plays an anti-apoptotic role upstream of capsase-9.

Functional analysis in these clones is summarized in Fig. 6B. The hypoxic inducibility in HIF-1α-overexpressing and dn HIF-1α clones was 8.4 ± 0.4- and 0.7 ± 0.1-fold, respectively, as compared to 3.8 ± 0.4-fold in control IRPTCs. Of interest, HIF-1α overexpressing clones showed a significantly higher luciferase activity even in normoxic conditions (3.6 ± 0.8-fold vs control normoxic IRPTCs).

With the overexpression clones, we checked Bax mRNA expression in normoxic and hypoxic conditions. However, as seen in Fig. 6C, the amount of Bax mRNA was unaffected by the expression level of HIF-1α in both normoxic and hypoxic conditions. Furthermore, the expression level of HIF-1α did not relate to the difference in death profile under hypoxia (data not shown). Thus, we conclude that Bax mRNA is not upregulated in IRPTC by HIF-1 and that induction of HIF-1 does not affect death profile at the permissive temperature.

Treatment at the nonpermissive temperature renders IRPTC susceptible to HIF-induced Bax mRNA upregulation, a possible role of p53

Based on these findings, we sought to determine whether the unaffected amount of Bax mRNA was due to the nature of proximal tubular cell itself or could be ascribed to the immortalization process by introducing temperature-sensitive SV40 large T antigen. To this end, we cultured IRPTCs under nonpermissive (40 °C) conditions, in which IRPTC is expected to revert to its untransformed phenotype [26,27]. Fig. 7A shows the relative amount of p53 in transformed (permissive) and untransformed (nonpermissive) conditions. The band of p53 is apparently weaker when cultured at 40 °C than at 37 °C. Considering that SV 40 large T antigen modulates the intracellular environment partly by binding and inactivating the cellular proteins such as pRB and p53, we can speculate that the entrapped, functionally inactive p53 is released from the SV40 large T antigen and regains its native function at the nonpermissive temperature. With these conditions, we examined changes in Bcl2 and Bax mRNA by hypoxia (Figs. 7B and C). Bcl2 mRNA was decreased to 0.36-fold by hypoxia, as seen in permissive conditions. On the other hand, Bax mRNA was markedly increased to 2.3-fold, in contrast to lack of quantitative changes in permissive conditions. To further strengthen the hypothesis that HIF-1 upregulates Bax mRNA expression, we performed similar experiments using stable clones carrying dominant-negative (dn) HIF-1α. While Bcl2 mRNA was similarly decreased to 0.39-fold, Bax mRNA was decreased by hypoxic stimulation, although the difference did not reach statistical significance (0.59-fold, $p = 0.054$). The resultant Bax/Bcl2 ratio is shown in Fig. 7D. In nonpermissive conditions, the ratio was increased more prominently (6.4-fold) by hypoxia than in permissive conditions (5.7-fold), which was abrogated in dn HIF-1α expressing clones. A casual effect by the integration site of the transgene was unlikely because the relatively higher Bcl2 and Bax mRNA expression in the normoxic dn HIF-1α clone was also observed using other dominant-negative clones.

Taken together, we propose the possibility that in untransformed proximal tubular cells, HIF-1 might be

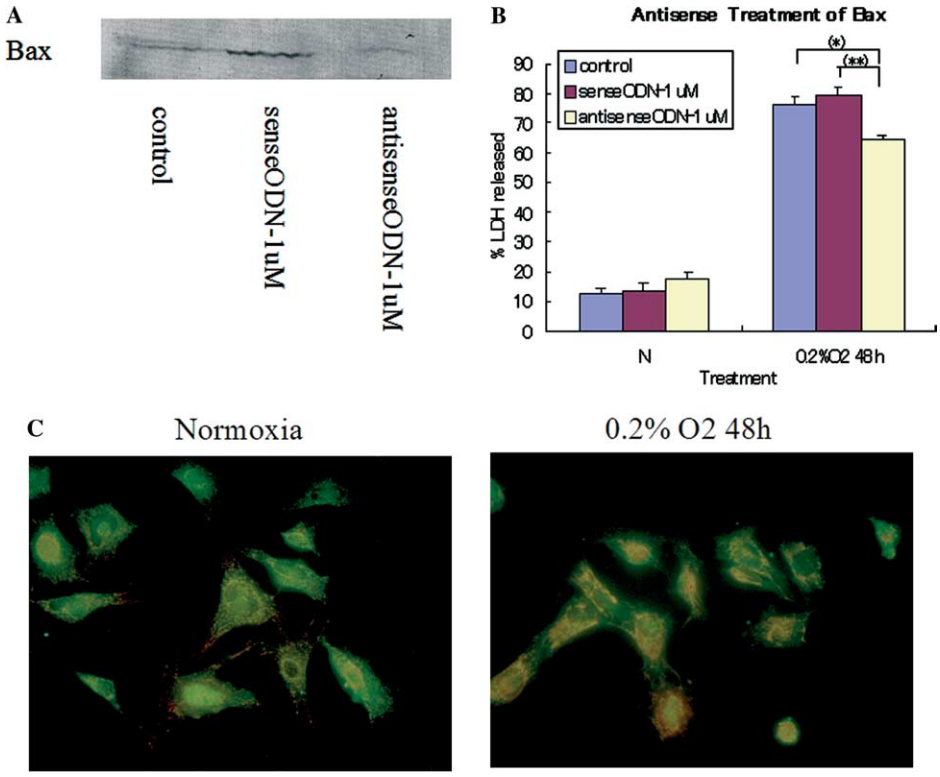

Fig. 5. Effects of antisense ODN treatment against Bax. A pro-apoptotic function of Bax was determined by introducing antisense oligonucleotides (ODNs). (A) After 48 h of antisense ODN delivery by cationic liposome, the amount of Bax protein was evaluated by Western blotting. The amount of Bax was reduced significantly in antisense ODN group as compared to control and sense ODN groups, indicating an effective inhibition of Bax by this method. (B) Using these ODNs, we examined the effect on cell death by inhibiting Bax expression. LDH assays showed that treatment with an antisense ODN resulted in a mild, but constant reduction in the number of dead cells ($65.0 \pm 1.0\%$), as compared to control ($76.1 \pm 3.2\%$, $p = 0.043$) and sense ODN ($79.3 \pm 2.6\%$, $p = 0.0005$) groups. These results confirm that Bax also plays a central role in hypoxia-induced tubular cell apoptosis, although the amount of Bax mRNA was unaffected by hypoxia (Fig. 2B). The proportion of dead cells is higher compared to those in Figs. 1A and B, since LDH assays include both apoptotic and necrotic dead cells (representative of three independent experiments with the n number of 8, $^{*}p < 0.05$, $^{**}p < 0.01$). (C) Immunohistochemical analysis revealed translocation of Bax from the cytosol to mitochondria following hypoxic stimulation. Both normoxic and hypoxic IRPTCs were double-stained with anti-Bax antibody and MitoTracker, whereby the obviously yellowish signals were detected around the nucleus in some cells of hypoxia-treated groups, while these signals were not apparent in normoxic controls. The yellow signal indicates the computer-assigned colocalization of red (MitoTracker) and green (Oregon Green 488). Negative controls included omission of the incubation step with the primary antibody, which revealed no positive staining (600×). (For interpretation of the references to colour in this figure legend, the reader is referred to the web version of this article.)

working upstream of Bax to enhance its expression, at least partly, through p53-dependent mechanisms.

Discussion

These results demonstrate that hypoxia induces apoptosis in IRPTC in vitro based on molecular and morphological criteria. In our experimental conditions, severe hypoxia (0.2% O_2) induced more apoptosis as compared to mild to moderate hypoxia (1% O_2). In general, severe hypoxia is associated with necrosis rather than apoptosis, and the clear distinction between apoptosis and necrosis is at times difficult. In addition, results of assays for apoptosis are not infrequently equivocal [33]. Considering the limitations of these methods, the results of our studies taken together are sufficient for us to conclude that apoptosis plays a certain role in hypoxia-associated proximal tubular cell injury. Similar results were previously reported by Santore et al. [34], who established a role for apoptosis in the lung epithelial cell line A549 under anoxic conditions.

Employing quantitative real-time PCR analysis, we demonstrated a time-dependent downregulation of the mitochondrial anti-apoptotic gene, Bcl2, while the expression of Bax, a pro-apoptotic one, remained constant. In chemical hypoxia such as ATP depletion, a similar disturbance in Bcl2–Bax axis has been described in various in vitro experiments [35,36]. Under hypoxic stimulation, Bcl2 expression decreases, while Bax translocates to the mitochondria, thus conferring the apoptotic death signal. Our results would support this mechanism.

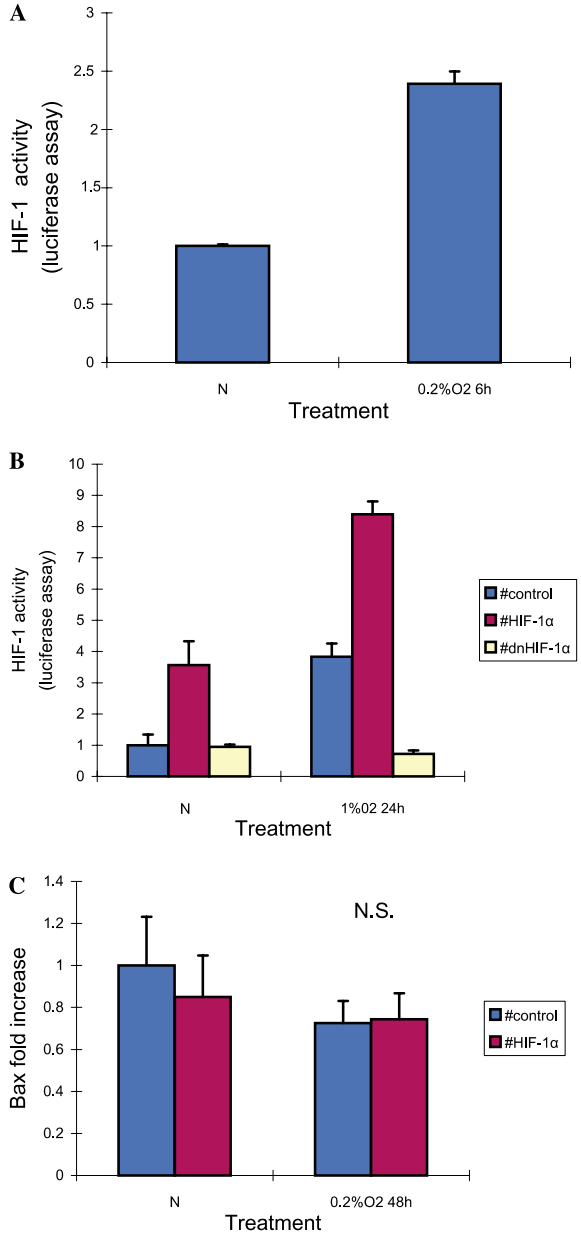

Fig. 6. HIF-1α is induced by hypoxia in IRPTC, but does not affect Bax expression. (A) Relative HIF-1 activity measured by luciferase assays. The hypoxic inducibility of HRE-driven luciferase activity was measured in IRPTC. When we cultured IRPTCs in 0.2% O_2 for 6 h, the hypoxic inducibility of the firefly luciferase was 2.4 ± 0.1-fold, indicating that HIF-1 is activated in 0.2% O_2 in IRPTC. In these experiments, IRPTCs were subjected to hypoxia for up to 6 h to minimize the detrimental effect of reduced cell viability ($n = 3$). (B) We constructed stable clones carrying HIF-1α and dominant-negative (dn) HIF-1α to clarify a role of HIF-1 on Bax transcription. Functional analysis in these clones was performed measuring hypoxic inducibility of HRE-luciferase. The hypoxic inducibility in HIF-1α-overexpressing and dn HIF-1α clones was 8.4 ± 0.4- and 0.7 ± 0.1-fold, respectively, as compared to 3.8 ± 0.4-fold in control IRPTCs. It should also be noted that HIF-1α overexpressing clones exhibited a significantly higher luciferase activity even in normoxic conditions (3.6 ± 0.8-fold vs control normoxic IRPTCs) ($n = 3$). (C) Using these overexpression clones, we checked Bax mRNA expression. The amount of Bax mRNA was unaffected by the expression level of HIF-1α in both normoxic and hypoxic conditions ($n = 3$, real-time PCR).

In cells undergoing apoptosis through mitochondrial pathways, a decrease in Bcl2 leads to mitochondrial membrane instability and cytochrome *c* release into the cytosol, with subsequent activation of caspase-9 and endonucleases, resulting in internucleosomal DNA fragmentation. All of these events occurred coordinately in IRPTC under severe hypoxia, and overexpression of Bcl2 ameliorated this process, consistent with the previous reports in various cell lines [37–39]. Likewise, inhibition of Bax by antisense ODN reduced hypoxia-induced IRPTC injury. These findings strongly suggest that tubular cell apoptosis occurs, at least in part, via mitochondrial signaling pathways.

Studies investigating upstream signaling molecules of Bcl2 and Bax advocate a concept that HIF-1 induced by hypoxia stabilizes p53 and resultantly transactivates Bax mRNA expression, but the results were dependent on the cell types [22] or experimental conditions [23,24]. In view of those controversies whether HIF-1 could contribute to the elevated expression of Bax in hypoxic conditions, studies have been awaited to address that issue using renal proximal tubular cells, which are of the most susceptible portion of renal tubules against ischemic injury. In our experiments under permissive conditions, though, the upregulation of Bax was not observed at any time point during the hypoxic stimulation, despite that HIF-1α was induced significantly under conditions we employed. We assumed that the SV40 large T antigen induced by temperature-sensitive mutant virus might be interfering this process and then cultured IRPTCs in nonpermissive conditions. An SV40 large T antigen interacts with p53 at its core domain, thus inhibiting the sequence-specific transactivation [40] of p53. In addition, disappearance of SV40 large T antigen and reversion to the normal phenotype are well related to the gain of function of p53 and its sequence-specific transactivation [41]. As a result, we found out for the first time that, under nonpermissive conditions, Bax mRNA was upregulated significantly in IRPTC by hypoxia, which was abrogated by inhibiting HIF-1 activity. These findings raise the possibility that HIF-1 might be upregulating Bax mRNA through p53, at least in part, in untransformed proximal tubular cells and that the enhanced amount of Bax is not an essential part of hypoxia-induced tubular cell apoptosis, since IRPTCs proceeded to apoptosis through the translocation of Bax even in permissive conditions where p53 is expected to be inactive in large part.

In summary, we demonstrated that hypoxia induces apoptosis, along with necrosis, in IRPTC through the decreased expression of Bcl2 mRNA and the elevated caspase-9 activity downstream, all characteristic of apoptotic cell death mediated by the mitochondrial pathways. Both overexpression of Bcl2 and inhibition of Bax ameliorated the above process. And as an upstream signaling molecule of Bax, it was speculated that HIF-1

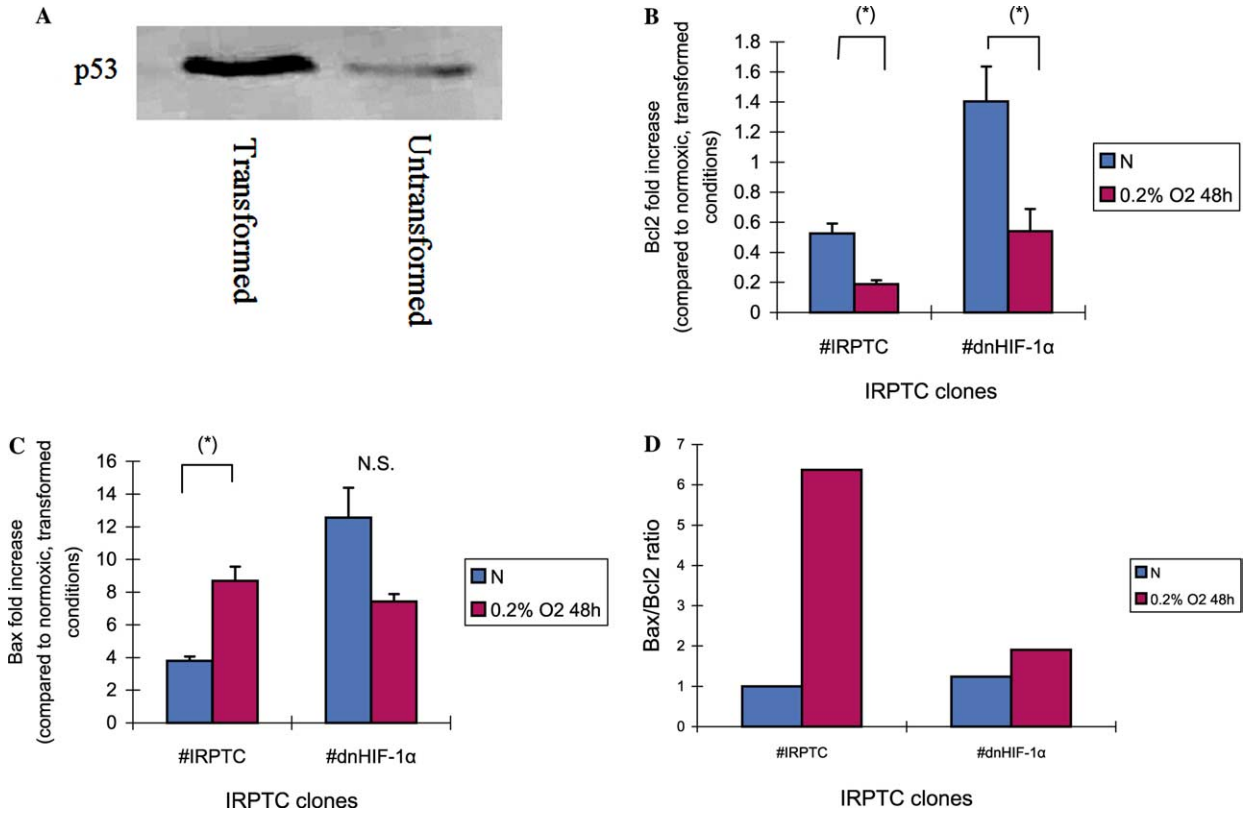

Fig. 7. Reversion to the untransformed phenotype renders IRPTC susceptible to hypoxia-induced upregulation of Bax. (A) The relative amount of p53 protein in transformed (permissive) and untransformed (nonpermissive) conditions. The band of p53 is apparently weaker when cultured at 40 °C than at 37 °C, which indicates that the functionally inactive p53 is released from the SV40 large T antigen and regains its native function at the nonpermissive temperature. (B,C) With these conditions, we examined changes in Bcl2 and Bax mRNA by hypoxia. Bcl2 mRNA was decreased to 0.36-fold by hypoxia, as was observed in permissive conditions. Bax mRNA, however, was markedly increased to 2.3-fold, while unchanged in permissive conditions. To clarify the possible role for HIF-1 in this context, we performed similar experiments utilizing clones carrying dominant-negative (dn) HIF-1α. While Bcl2 mRNA was similarly decreased to 0.39-fold, Bax mRNA was unaffected, or even decreased, by hypoxic stimulation (0.59-fold, $p = 0.054$). These results obviously show that HIF-1 is a contributory factor to Bax mRNA upregulation and that p53 is most likely a co-working factor during the process ($n = 3$, real-time PCR, $^{*}<0.05$). (D) The resultant Bax/Bcl2 ratio. At the nonpermissive temperature, the ratio was increased more prominently (6.4-fold) by hypoxia than at the permissive temperature (5.7-fold), whereas such changes were absent in dn HIF-1α expressing clones.

was working synergistically with p53 to upregulate Bax mRNA in proximal tubular cells of normal phenotype, while the enhanced Bax was not an indispensable part of its death execution, as shown in transformed IRPTCs.

Chronic hypoxia in the tubulointerstitium stays as part of the final common pathways in progressive renal disease. Further investigations on the apoptotic mechanisms focusing on the mitochondrial pathways will lead us to better understanding of the progressive hypocellular fibrosis in chronic hypoxic kidneys.

Acknowledgments

This work was supported by Grants in Aid for Scientific Research from the Ministry of Education, Science and Culture (#13671100) and from the Japanese Ministry of Health and Welfare (H13-21th century-17). We thank Dr. Jeremy Hughes (University of Edinburgh, UK) for helpful discussions and comments. We also thank Dr. Kiyoshi Kurokawa, Dr. Toshio Miyata, and Dr. Reiko Inagi (Tokai University, Kanagawa, Japan) for many helpful advices and generous support.

References

[1] H.R. Jacobson, Lancet 338 (1991) 419–423.
[2] A. Bohle, G. Kressel, C.A. Muller, G.A. Muller, Pathol. Res. Pract. 185 (1989) 421–440.
[3] L.G. Fine, D. Bandyopadhay, J.T. Norman, Kidney Int. Suppl. 75 (2000) S22–S26.
[4] J. Hughes, Nephrol. Dial. Transplant. 15 (Suppl. 6) (2000) 55–57.
[5] M. Schumer, M.C. Colombel, I.S. Sawczuk, G. Gobe, J. Connor, K.M. O'Toole, C.A. Olsson, G.J. Wise, R. Buttyan, Am. J. Pathol. 140 (1992) 831–838.
[6] A. Shimizu, N. Yamanaka, Virchows Arch. B Cell. Pathol. Incl. Mol. Pathol. 64 (1993) 171–180.
[7] G. Wiegele, M. Brandis, L.B. Zimmerhackl, Nephrol. Dial. Transplant. 13 (1998) 1158–1167.
[8] W. Lieberthal, S.A. Menza, J.S. Levine, Am. J. Physiol. 274 (1998) F315–327.
[9] L.R. Feldenberg, S. Thevananther, M. del Rio, M. de Leon, P. Devarajan, Am. J. Physiol. 276 (1999) F837–F846.
[10] M. Brezis, P. Shanley, P. Silva, K. Spokes, S. Lear, F.H. Epstein, S. Rosen, J. Clin. Invest. 76 (1985) 1796–1806.
[11] Y. Tsujimoto, J. Cossman, E. Jaffe, C.M. Croce, Science 228 (1985) 1440–1443.

[12] K.G. Wolter, Y.T. Hsu, C.L. Smith, A. Nechushtan, X.G. Xi, R.J. Youle, J. Cell Biol. 139 (1997) 1281–1292.
[13] A. Gross, J. Jockel, M.C. Wei, S.J. Korsmeyer, EMBO J. 17 (1998) 3878–3885.
[14] Y. Tsujimoto, S. Shimizu, FEBS Lett. 466 (2000) 6–10.
[15] J.C. Reed, Oncogene 17 (1998) 3225–3236.
[16] J.M. Adams, S. Cory, Science 281 (1998) 1322–1326.
[17] T.G. Graeber, J.F. Peterson, M. Tsai, K. Monica, A.J. Fornace Jr., A.J. Giaccia, Mol. Cell. Biol. 14 (1994) 6264–6277.
[18] C. Yin, C.M. Knudson, S.J. Korsmeyer, T. Van Dyke, Nature 385 (1997) 637–640.
[19] M.E. McCurrach, T.M. Connor, C.M. Knudson, S.J. Korsmeyer, S.W. Lowe, Proc. Natl. Acad. Sci. USA 94 (1997) 2345–2349.
[20] T. Miyashita, J.C. Reed, Cell 80 (1995) 293–299.
[21] J.P. Piret, D. Mottet, M. Raes, C. Michiels, Biochem. Pharmacol. 64 (2002) 889–892.
[22] Q. Zhan, S. Fan, I. Bae, C. Guillouf, D.A. Liebermann, P.M. O'Connor, A.J. Fornace Jr., Oncogene 9 (1994) 3743–3751.
[23] X. Long, M.O. Boluyt, M.L. Hipolito, M.S. Lundberg, J.S. Zheng, L. O'Neill, C. Cirielli, E.G. Lakatta, M.T. Crow, J. Clin. Invest. 99 (1997) 2635–2643.
[24] K.A. Webster, D.J. Discher, S. Kaiser, O. Hernandez, B. Sato, N.H. Bishopric, J. Clin. Invest. 104 (1999) 239–252.
[25] S.S. Tang, F. Jung, D. Diamant, D. Brown, D. Bachinsky, P. Hellman, J.R. Ingelfinger, Am. J. Physiol. 268 (1995) F435–F446.
[26] J.Y. Chou, Methods Enzymol. 109 (1985) 385–396.
[27] S. Ray, M.E. Anderson, P. Tegtmeyer, J. Virol. 70 (1996) 7224–7227.
[28] N. Hanafusa, Y. Yatomi, K. Yamada, Y. Hori, M. Nangaku, T. Okuda, T. Fujita, K. Kurokawa, M. Fukagawa, Nephrol. Dial. Transplant. 17 (2002) 580–586.
[29] T. Sato, M.G. van Dixhoorn, W.E. Schroeijers, L.A. van Es, M.R. Daha, Kidney Int. 51 (1997) 173–181.
[30] M.W. Halterman, C.C. Miller, H.J. Federoff, J. Neurosci. 19 (1999) 6818–6824.
[31] I. Otter, S. Conus, U. Ravn, M. Rager, R. Olivier, L. Monney, D. Fabbro, C. Borner, J. Biol. Chem. 273 (1998) 6110–6120.
[32] A.P. Levy, N.S. Levy, S. Wegner, M.A. Goldberg, J. Biol. Chem. 270 (1995) 13333–13340.
[33] N. Ueda, P.D. Walker, S.M. Hsu, S.V. Shah, Proc. Natl. Acad. Sci. USA 92 (1995) 7202–7206.
[34] M.T. Santore, D.S. McClintock, V.Y. Lee, G.R. Budinger, N.S. Chandel, Am. J. Physiol. Lung. Cell. Mol. Physiol. 282 (2002) L727–L734.
[35] Y. Wang, A.A. Knowlton, T.G. Christensen, T. Shih, S.C. Borkan, Kidney Int. 55 (1999) 2224–2235.
[36] P. Saikumar, Z. Dong, Y. Patel, K. Hall, U. Hopfer, J.M. Weinberg, M.A. Venkatachalam, Oncogene 17 (1998) 3401–3415.
[37] S. Shimizu, Y. Eguchi, H. Kosaka, W. Kamiike, H. Matsuda, Y. Tsujimoto, Nature 374 (1995) 811–813.
[38] M.D. Jacobson, M.C. Raff, Nature 374 (1995) 814–816.
[39] E. Peherstorfer, B. Mayer, S. Boehm, A. Lukas, P. Hauser, G. Mayer, R. Oberbauer, Am. J. Physiol. Renal. Physiol. 283 (2002) F190–F196.
[40] K. Segawa, A. Minowa, K. Sugasawa, T. Takano, F. Hanaoka, Oncogene 8 (1993) 543–548.
[41] W.S. el-Deiry, J.W. Harper, P.M. O'Connor, V.E. Velculescu, C.E. Canman, J. Jackman, J.A. Pietenpol, M. Burrell, D.E. Hill, Y. Wang, et al., Cancer Res. 54 (1994) 1169–1174.